Available online at www.sciencedirect.com
ScienceDirect
International Journal of Mass Spectrometry 269 (2008) 149–164
International Journal of Mass Spectrometry
www.elsevier.com/locate/ijms

Theoretical study of through-space and through-bond electron transfer within positively charged peptides in the gas phase

Monika Sobczyk, Diane Neff, Jack Simons *

Chemistry Department and Henry Eyring Center for Theoretical Chemistry, University of Utah, Salt Lake City, UT 84112, United States

Received 12 July 2007; received in revised form 2 October 2007; accepted 4 October 2007
Available online 18 October 2007

Abstract

As part of an on-going effort to probe mechanisms for disulfide and backbone N–C_α cleavage under electron capture or electron-transfer dissociation mass spectroscopy conditions, theoretical simulations have been carried out to consider the probabilities that

a. an electron initially attached to a protonated amine site on a side chain can migrate (through-bond or through-space) to an S–S σ* orbital and thus cause disulfide cleavage;
b. an electron initially attached to a protonated site might be transferred (through-bond or through-space) to another protonated site or to a fixed-charge positive site thus allowing the electron to migrate throughout charged sites in a multiply charged peptide.

The primary findings of this work include:

c. charged-site to S–S σ* orbital through-bond electron transfer can occur at significant probabilities but only over ca. 5 intervening bonds covering up to ca. 15 Å;
d. through-space electron transfer from protonated sites to protonated sites or from fixed-charge sites to fixed-charge sites can be facile, but between protonated and fixed-charge sites transfer is very slow; to effect the transfers between equivalent sites, the two sites must come within ca. 5 Å of one another;
e. through-space electron transfer from a protonated or fixed-charge site to an S–S σ* orbital can occur with reasonable probability but if the two sites come within ca. 5 Å of one another.

Based on these findings, speculation is offered both to interpret recent findings of the McLuckey group on flexible, triply charged peptides and earlier data from the Marshall group on more rigid, helical, doubly charged peptides, both of which contain disulfide linkages that experiments find to be readily cleaved.

Keywords: Electron-transfer dissociation; Disulfide cleavage; Electron transfer

1. Introduction

Electron-capture dissociation [1] (ECD) and electron-transfer dissociation [2] (ETD) mass spectroscopic methods have shown much utility and promise for sequencing peptides and proteins. A strongpoint of both techniques is their propensity for selectively cleaving disulfide and N–C_α bonds and for doing so over a wide range of the backbone, thus producing many different fragment ions. Parallel with many advances in the experimental development and improvement of these methods, theoretical studies have been carried out to try to determine the mechanism(s) [3,20] by which electron attachment leads to these bond cleavages.

In this paper, some of the proposed mechanisms are reviewed and experimental evidence that may help differentiate among them is discussed. Then, results of new experiments from the McLuckey lab [4] are briefly introduced as motivation for the present theoretical study on how electrons initially attached to a

* Corresponding author.
E-mail address: simons@chem.utah.edu (J. Simons).

1387-3806/$ – see front matter © 2007 Elsevier B.V. All rights reserved.
doi:10.1016/j.ijms.2007.10.003

multiply positively charged gas-phase peptide ion may migrate from the site of initial attachment to other sites (including other positive sites and disulfide bonds) within the peptide. Having some idea of how facile various intramolecular electron migration steps are should prove of substantial help in synergistic experimental–theoretical studies of the mechanisms of ECD/ETD.

In the following subsection, the most commonly supported mechanisms are briefly overviewed. In Section 2, the new McLuckey experiments are discussed and the need for studying intramolecular electron transfer is introduced. Section 3 describes the theoretical methods used. Section 4 contains the results and discussion of their meaning, and Section 5 offers a summary of the primary findings as well as possible rationalizations of the experiments based upon the theoretical findings reported here.

1.1. The Coulomb-assisted direct-attachment mechanism

In earlier efforts [3g–3l,3n] to explore how low-energy electrons can cleave S–S or N–C_α bonds in positively charged gas-phase peptides (e.g., as exist under electrospray conditions in mass spectroscopy experiments), we proposed that electrons can attach directly to S–S σ* or OCN amide π* orbitals, but only under special conditions. In particular, we suggested that such low-lying empty orbitals can have their energies even further lowered by attractive Coulomb interactions with one or more positively charged groups (e.g., protonated amine or fixed-charge groups on side chains) thus rendering exothermic direct electron attachment. In Scheme 1, we illustrate the mechanisms by which such electron attachment events are proposed to lead to cleavage of disulfide or N–C_α bonds.

After attaching to an S–S σ* orbital, cleavage of the disulfide bond is prompt. However, subsequent to attaching to an amide π* orbital, a barrier (ca. 30 kcal mol^{-1}) must still be surmounted to cleave the N–C_α bond, after which a proton transfer forms the characteristic c and z fragments shown in Scheme 1.

We know from past work on dissociative electron attachment [5] that, in the absence of Coulomb stabilization, vertical electron attachment to an S–S σ* or amide π* orbital is ca. 1 eV and ca. 2.5 eV endothermic, respectively. The Coulomb potential varies with distance R (Å) as 14.4 eV Å/R (Å), so we predicted under what structural circumstances such direct electron attachment should be expected. For example, we proposed that a disulfide linkage must experience Coulomb stabilization exceeding 1 eV to render our direct-attachment mechanism feasible; this stabilization could, for example, arise from a single positively charged site closer than ca. 14 Å, from two positive sites each 7 Å distant, or from a doubly charged site 28 Å away. We also predicted that a single positive charge 14.4/2.5 = 6 Å from an OCN π* orbital could render this orbital amenable to exothermic direct electron attachment.

1.2. Suggestive early experiments

Electron-capture dissociation (ECD) experiments from the Marshall group [6] on synthetic peptides $(AcCA_nK+H)_2^{2+}$,

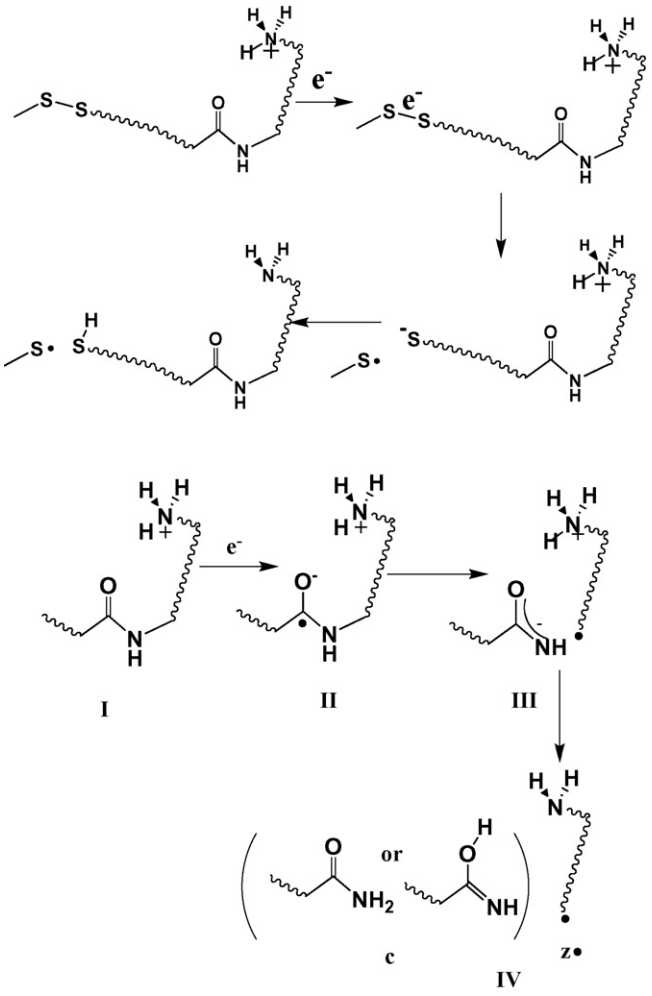

Scheme 1. Direct electron attachment to Coulomb stabilized S–S σ* or OCN π* orbital to cleave disulfide or N–C_α bonds.

with n = 10, 15, 20, showed significant disulfide cleavage even for the n = 20 species in which the two positively charged Lys residues' charge sites are thought to be ca. 30 Å from the S–S bond. The gas-phase structure of such dications, deduced from ion mobility measurements [7] and molecular dynamics simulations, is shown in Fig. 1 for the n = 15 case. In these same experiments, some N–C_α bond cleavage was also observed, but only within the four alanines closest to a positively charged Lys terminus. N–C_α bond cleavage of other alanine units did not occur to any appreciable extent. Assuming the helical structure shown in Fig. 1, the four alanines within which N–C_α cleavage occurs reside within ca. 6 Å of the nearest Lys' positively

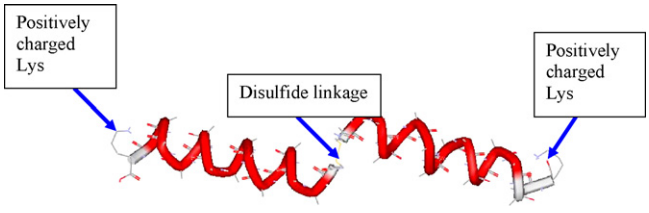

Fig. 1. Assumed structure of doubly charged $(AcCA_{15}K+H)_2^{2+}$ cations in gas phase (redrawn from Ref. [3i]).

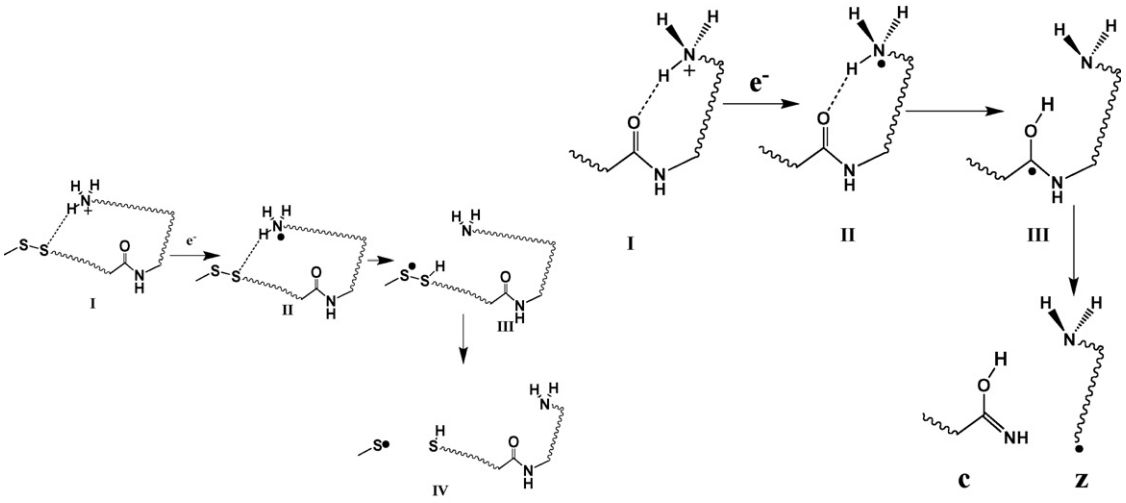

Scheme 2. Hydrogen atom transfer mechanism for disulfide and N–C_α cleavage.

charged nitrogen center so their cleavage is consistent with the Coulomb stabilization model.

The significance of the experimental findings just briefly described is that they are difficult to explain within the framework of an alternative earlier mechanism for S–S and N–C_α cleavage that is outlined in Scheme 2.

1.3. The hydrogen atom mechanism

In this mechanism [1a], an electron is captured at a protonated site to form a hypervalent radical. This radical then loses an H atom, which attacks either an S–S bond (to cleave it promptly) or a carbonyl oxygen (to form an HO–C•–NH–C_α radical). The HO–C•–NH–C_α radical subsequently undergoes N–C_α bond cleavage after surmounting a barrier. A main difference between the hydrogen atom mechanism shown in Scheme 2 and the Coulomb-assisted electron attachment mechanism of Scheme 1 is that the former requires that the positive site be close enough to the S–S or N–C_α bond to be cleaved to allow the hydrogen atom released by the hypervalent radical to reach this bond. For the species shown in Fig. 1, it is difficult to imagine how a hydrogen atom released from one of the Lys termini can "find" an S–S bond that is ca. 30 Å away (as is the case for $n = 20$). It is even difficult to understand how such a hydrogen atom can find and attack a carbonyl oxygen that has four other amino acids between the source of the hydrogen atom (the Lys' terminal nitrogen) and this C=O group. In contrast, the Coulomb stabilization model's predictions have no difficulty rationalizing such findings as explained above.

It should be noted that ECD experiments were also carried out in the Marshall group [6] on species such as $(AcCA_{10}–NH_2 + Na)_2^{2+}$ which are thought to be unable to generate hydrogen atoms when electrons attach to the sodiated positive termini. However, S–S cleavage was observed to occur for such species in the Marshall-group experiments. This provides even more evidence that it is not essential for charge sites to be very close (e.g., within hydrogen-bonding distance) to S–S or carbonyl bonds or to involve protonation to realize disulfide or N–C_α bond cleavage.

The above discussion is not meant to suggest that the hydrogen atom mechanism is never operative in some cases. It may be that, when a protonated side chain is within hydrogen-bonding distance of an S–S bond or an amide carbonyl group, a mechanism such as shown in Scheme 2 can indeed be operative. The above discussion is meant to suggest that, when the positive site(s) are further away, disulfide and N–C_α cleavage can still occur via the mechanism shown in Scheme 1 because Coulomb stabilization can be operative over significantly longer distances (e.g., 14 Å for S–S cleavage; 6 Å for N–C_α cleavage) than characterize hydrogen bonding. So, our findings do not exclude the possibility that the mechanism of Scheme 2 is operative; they only suggest that a mechanism such as shown in Scheme 1 can also be involved.

1.4. Relative probabilities for electron attachment to positive sites and Coulomb-stabilized bond sites

Some time ago, we also carried out molecular dynamics simulations [3g,3h] in which model positively charged compounds containing disulfide bonds or N–C_α linkages and a protonated amine site were allowed to undergo charge transfer collisions with an anion (the small CH_3^- anion was used to avoid significant effects from steric crowding) having a small electron binding energy. We made use of Landau–Zener (LZ) theory to estimate the probabilities, cross-sections, and rates for two processes:

i. electron transfer to the protonated amine site's ground- or excited-Rydberg orbital to form a hypervalent species; and
ii. direct electron transfer to the S–S σ* or amide π* orbital to initiate bond cleavage.

These studies showed that the cross-section and probability for electron transfer to the positively charged site is one to

two orders of magnitude larger than for transfer to either the S–S σ* or amide π* orbital. Thus, it appears that the majority of the charge-reduction events (i.e., electron capture in ECD or electron transfer from an anion as in electron-transfer dissociation (ETD)) involve capture of an electron at a positive site. This would suggest that, when protonated sites are within hydrogen-bonding distance of an S–S bond or carbonyl oxygen, the mechanism of Scheme 2 could be dominant. Nevertheless, our molecular dynamics studies also showed that it is also possible for an electron to directly attach to a σ* or π* orbital that is Coulomb-stabilized.

Thus, we currently believe that disulfide and N–C_α bond cleavage in ECD and ETD can occur by either the hydrogen atom (e.g., for bonds very close to protonated side chains) or Coulomb-assisted direct-attachment mechanism (even for bonds more distant from charged sites and independent of the nature of the charge carrier). However, another possibility was raised by very recent work from the McLuckey lab [4] that we discuss in Section 2: that an electron may initially attach to a positive site but subsequently migrate from this site to an S–S σ* or amide π* orbital thus effecting disulfide or N–C_α cleavage much like shown in Scheme 1.

2. Possibilities for electron transfer after attachment and more recent experiments

2.1. Our earlier studies of through-bond (TB) electron transfer probabilities

When, in earlier work, we studied the disulfide and N–C_α cleavages observed in the species shown in Fig. 1, we wanted to know whether an electron initially attached to a positively charged Lys terminus could subsequently migrate to an amide π* or disulfide σ* orbital located down the helical chain. So, in earlier work [8], we also considered the possibility that an electron could undergo *through-bond* (TB) electron transfer to migrate to an S–S σ* or amide π* orbital. In particular, we used a protonated amine group $–NH_3^+$ as the model for the positive site and methylene groups $–(CH_2)_n–$ as the "spacers" separating the $–NH_3^+$ and the disulfide or amide unit. In Fig. 2, we show the ground- and excited-Rydberg [9] and S–S σ* orbitals of $H_3C–S–S–(CH_2)_n–NH_3^+$ for 1, 2, and 3 methylene spacer units. In these studies the $–(CH_2)_n–$ backbone was held rigid to keep the distance between the nitrogen atom and the closest sulfur atom fixed. Doing so allowed us to determine the dependence of the TB transfer rates with distance.

In these and other orbital plots shown in this paper, 70% of the total electron density is included within the outermost contour line. It is important to notice how the Rydberg orbitals have appreciable spatial overlap (most for the $n = 1$ compound and less as n increases) with the S–S σ* orbital because it is through such contacts that the through-bond transfer takes place.

By calculating the energies of three electron-attached electronic states (i.e., with the electron in the S–S σ* orbital, in the ground-Rydberg orbital, or in the excited-Rydberg orbital) as functions of the S–S bond length, we were able to identify at what S–S bond lengths the S–S σ* curve crossed the ground- or excited-Rydberg curve. In Fig. 3, we show an example of such plots for the species $H_3C–S–S–(CH_2)_3–NH_3$ containing three methylene units. The plots for systems with one and two methylene spacer units are qualitatively similar except

i. as seen in Fig. 2, the σ* and Rydberg orbitals overlap more than in Fig. 3 because these orbitals are closer together;
ii. the S–S σ* curve lies lower in energy relative to the two Rydberg curves because the stabilizing internal Coulomb energy within the $H_3C–S–S–(CH_2)_3–NH_3^+$ ion-pair state is stronger when the σ* and Rydberg sites are closer as they are in the one- and two-methylene cases.

Having obtained plots of the energies as discussed above, we focused on the crossing regions (e.g., near S–S distances of 2.2 Å and 2.4 Å in Fig. 3) and computed the adiabatic energies of the two states near these avoided curve cross-

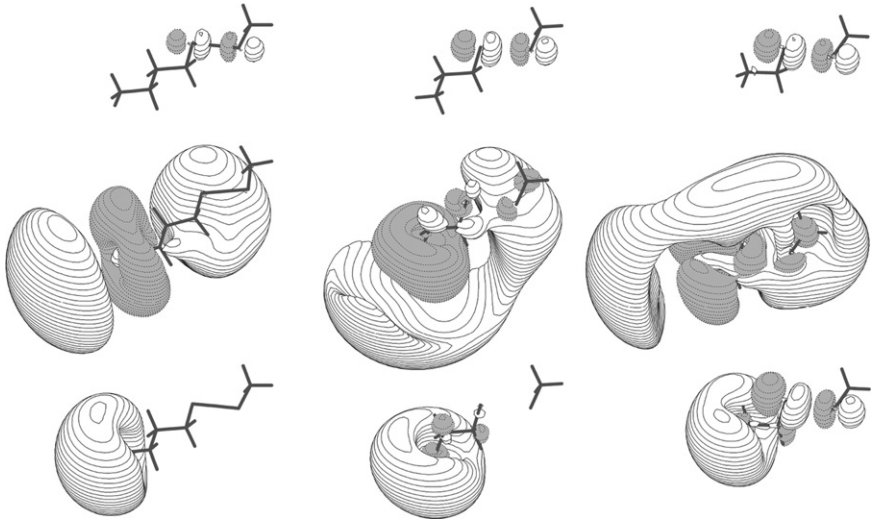

Fig. 2. Ground-Rydberg (lower), excited-Rydberg (middle), and S–S σ* orbitals for $H_3N^+–S–S–(CH_2)_n–CH_3$ model compounds for $n = 3$ (left), 2 (middle), and 1 (right) (redrawn from Refs. [8] and [12]).

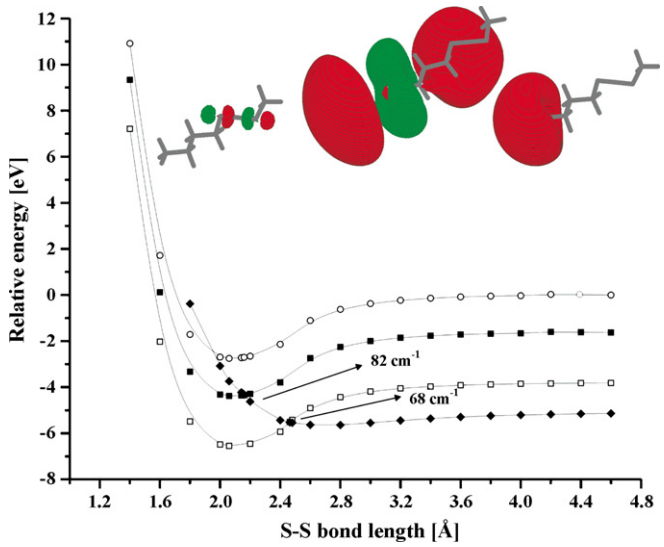

Fig. 3. Plots of the energies of $H_3C–S–S–(CH_2)_3–NH_3^+$ (open circles), ground-Rydberg (open squares) and excited-Rydberg [9] (filled squares) $H_3C–S–S–(CH_2)_3–NH_3$, and S–S σ*-attached $H_3C–S–S–(CH_2)_3–NH_3^+$ ion-pair (filled diamonds) states as functions of the S–S bond length.

ings. From the minimum-energy spacing of these two adiabatic states, we were able to obtain the Hamiltonian couplings $H_{1,2}$ pertinent to these state interactions (82 cm^{-1} and 68 cm^{-1} in Fig. 3). This process was repeated for the ground- and excited-Rydberg states' couplings with the S–S σ* states for each of the $H_3C–S–S–(CH_2)_{1–3}–NH_3$ cases.

In Fig. 4, we show plots of these $H_{1,2}$ couplings (in cm^{-1} units) as functions of the distance R between the midpoint of the S–S bond and the centroid of the (ground- or excited-Rydberg) orbital. These coupling strengths, via Landau–Zener (LZ) theory, allowed us to estimate the probabilities (for the $n = 1$, 2, and 3 compounds and for the ground- or excited-Rydberg state) for an electron to transfer from the Rydberg orbital to the S–S σ* orbital. These probabilities ranged from 0.004 (for the $n = 3$ compound) to 0.6 (for the $n = 1$ compound), and were larger for the excited-Rydberg state than for the ground-Rydberg state.

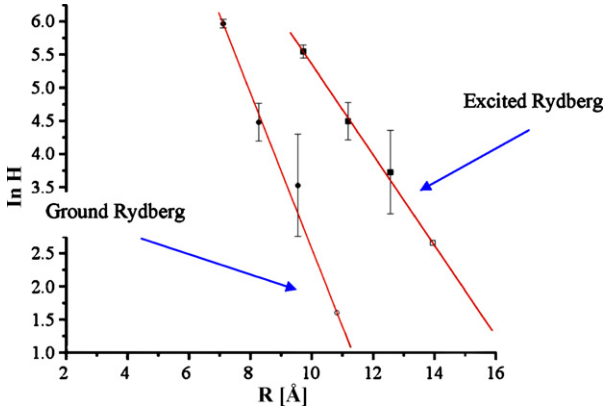

Fig. 4. Hamiltonian couplings $H_{1,2}$ (cm^{-1}) vs. distance R (Å) between midpoint of the S–S bond and the centroid of the ground- or excited-Rydberg orbital. The error bars correspond to estimated uncertainties of ±50 cm^{-1} in the computed $H_{1,2}$ values as cited in Ref. [8].

The $H_{1,2}$ couplings clearly display the expected exponential decay with distance. Their magnitudes decay to $H_{1,2}$ = ca. 55 cm^{-1} (or $\ln H_{1,2} = 4$) near 9 Å for the ground-Rydberg and near 12 Å for the excited-Rydberg orbitals, respectively. The relevance of noting over what range the couplings exceed this value is that, below this value, the probability of undergoing a through-bond electron transfer for the compounds discussed above falls to ca. 10^{-3}. In contrast, coupling strengths of ca. 500 cm^{-1} produce transfer probabilities exceeding 10%.

To estimate the rates at which such through-bond electron transfers occur, we multiplied the surface-hopping probabilities p discussed above by the frequency ν with which the avoided crossings (e.g., see Fig. 3) are encountered. These frequencies were estimated by multiplying the vibrational frequency ν_{SS} of the S–S bond by the thermal probability $P = \exp(-E^*/kT)/q_{vib.}$ that the S–S bond has sufficient energy E^* to access the crossing region ($q_{vib.}$ is the vibrational partition function for the S–S vibrational mode). If the crossing occurs in a region where zero-point vibration can access, P will be near unity. So, the rates (events per second) for Rydberg-to-σ* TB electron transfer were estimated as

$$\nu_{TB} = \nu_{SS} p P \quad (1)$$

In the through-space (TS) electron transfer studies carried out as part of the present effort, the surface-hopping probabilities p can be obtained using LZ theory as discussed above, but the frequencies ν for encountering the avoided crossing regions are evaluated in a different manner. For the TB case, the spacer backbone is held rigid, so the dynamical motion that causes the system to encounter a curve crossing is the S–S vibration. This is why the frequency of encountering a crossing is the S–S vibrational frequency attenuated by the thermal probability that this mode has adequate energy to access the crossing. In contrast, in the TS electron transfer processes, the rate limiting step in determining the frequency of encountering a crossing region is the frequency $\nu_{contact}$ with which the terminus of a side chain holding the attached electron moves into spatial contact with the S–S σ* orbital (or an amide π* orbital which we intend to study in a future work). To then evaluate the TS electron transfer rate, $\nu_{contact}$ is multiplied by the LZ surface-hopping probability p and by the probability P that the S–S bond has enough vibrational energy in it to access the crossing.

We will elaborate on the differences between ν_{SS} and $\nu_{contact}$ later when comparing the TB and TS transfer processes. Until then, it is useful to note that $\nu_{contact}$ is likely to be orders of magnitude smaller than ν_{SS} because for a terminus of a side chain to move into contact with the disulfide linkage located in the core of peptides such as studied in the McLuckey group requires much more complicated geometrical movements than a simple S–S vibrational motion.

2.2. New experiments suggesting intramolecular electron transfer

Quite recently, the McLuckey group performed a series of ETD experiments [4] on model multiply charged peptides con-

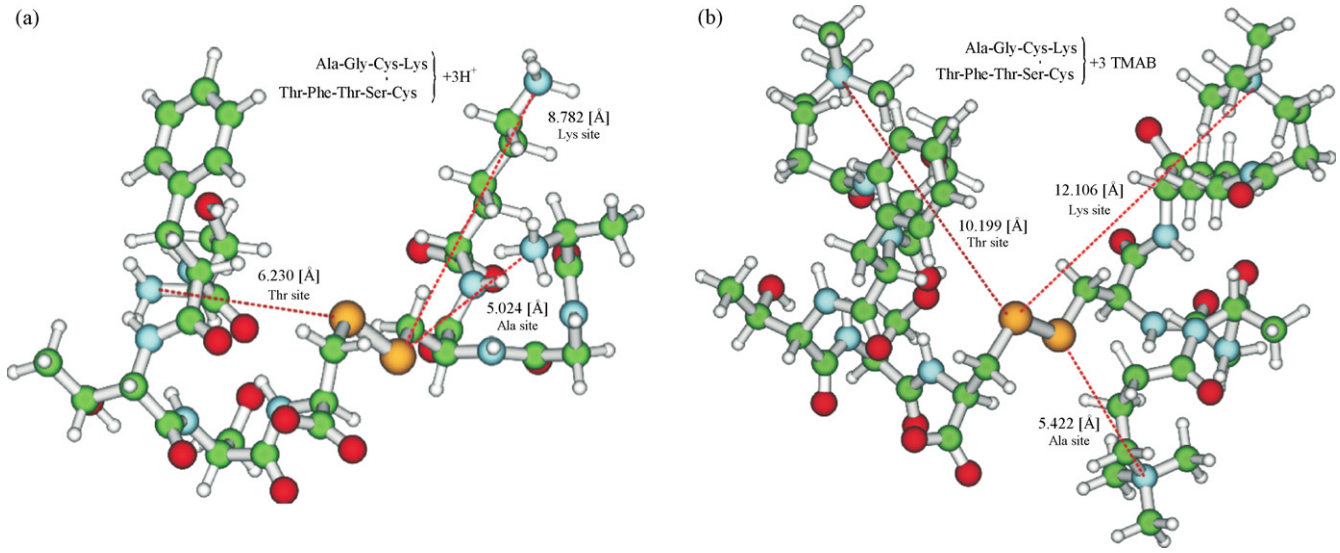

Fig. 5. Triply charged ions containing disulfide bond at the core with three arms whose termini can be protonated (a) or charged by adding TMAB to the Ala, Lys, and terminal Thr amines (b).

taining a disulfide linkage such as shown in Fig. 5a and b and denoted Ala-Gly-Cys(-Lys)-Cys-Ser-Thr-Phe-Thr. The amine sites on the Ala, Lys, and terminal Thr sites are protonated in the ion shown in Fig. 5a where their distances [10] to the disulfide linkage are also shown. In the ion shown in Fig. 5b, these three sites have been transformed into fixed-charge sites by chemically adding a unit denoted TMAB (replacing one hydrogen of an amine group by the $–C{=}O–(CH_2)_3–N(CH_3)_3^+$ group) to the nitrogen of their amines. So, in one compound, three protonated sites occur, while in the other, three fixed-charge sites occur. Of course, in the latter, the distances among the charged sites can be larger because of the extended TMAB group and, as shown in Fig. 5, the distances to the disulfide unit are considerably larger in the second compound. In these experiments, compounds in which one or two of the sites are protonated and two or one have fixed charge were also examined, but, because of limitations in the preparatory synthesis, it was not known which of the three sites were protonated and which held fixed charge.

The McLuckey group also studied another series of compounds, in which the Lys connected to the Cys is connected to a longer chain of amino acids and the overall species are quadruply charged. Although all of the discussion offered here is focused on the triply charged peptides shown in Fig. 5, the conclusions reached likely apply as well to the quadruply charged species.

All of the multiply charged cations shown in Fig. 5 can be viewed as consisting of a disulfide-linked core with three "arms" (Lys, Thr, and Ala) at the side-chain termini of which the positively charged groups reside. When an arm has been modified by TMAB, it is longer than when unmodified. It is useful to note that, even in the compound with three long arms (Fig. 5b), the charged sites are close enough to the S–S bond to render exothermic direct electron attachment to the S–S σ* orbital (i.e., the total Coulomb stabilization energy greatly exceeds 1 eV). It is also useful to notice that the distances between the positive sites and the disulfide linkage increase, when TMAB-substituted, considerably more for the Lys and Thr arms than for the Ala arm (compare distances in Fig. 5a and b). The latter observation will come into play when we attempt to rationalize the fragmentation propensities observed by the McLuckey group [4].

As the above ions undergo thermal motions in the gas-phase mass spectroscopy environment, the termini of their arms may come close to the S–S bond or to one another and thus allow the attached electron to migrate to another arm terminal site or to the S–S σ* orbital [11]. It is under such dynamical encounters that the kinds of electron transfer events studied in this work are suggested to occur. These encounters are what we earlier (see Section 2.2) termed contacts between the positive sites and one another or with the S–S bond.

One of the primary findings of the McLuckey-group experiments was that abundant fragment ions resulting from disulfide cleavage were observed even for the triply charged species (Fig. 5b) that contains no protonated amine sites; all three of its positive sites involved fixed charges that cannot liberate hydrogen atoms. This finding again suggests that something beyond the hydrogen atom mechanism of Scheme 2 can be operative, and it raises the question of to what extent direct attachment to the S–S σ* orbital occurs and to what extent attachment to a positive site followed by electron transfer to the S–S σ* orbital is operative.

Another observation in Ref. [4] was that the percent of fragmentation of the parent ion involving disulfide cleavage ranged from 68 to 80% for species as in Fig. 5a and for species containing one or three TMAB substitutions. The remaining fraction of fragment ions arose from backbone cleavage or side-chain loss. In contrast, the species containing two TMAB substitutions produced qualitatively less (36%) disulfide cleavage. In the latter compound, there are two long arms and one short arm, but, as noted earlier, synthetic limitations precluded knowing where the two TMAB substitutions exist. We will have more to say later about these puzzling findings (i.e., why do two TMAB

groups yield less disulfide cleavage but zero, one, or three give more?).

In interpreting their findings, the McLuckey group made some reasonable and intriguing mechanistic proposals including that

i. an electron initially attached to one of the positive sites (either protonated amine or fixed-charge) might be able to migrate to the S–S bond site and subsequently cleave the disulfide linkage; and
ii. an electron initially captured at one of the positive sites might be able to migrate to another positive site. These two possibilities are depicted qualitatively in Schemes 3 and 4, respectively.

For these two intramolecular electron transfer events, the possibilities that need to be considered include

a. an electron initially attached to a positive site might migrate, using the orbitals of the intervening "spacer" units, in a trough-bond manner to the disulfide linkage;
b. an electron initially attached to a positive site might migrate, when a Rydberg orbital at this site moves (due to the folding motion of the side-chain "arm" on which it resides) to directly overlap the S–S σ* orbital, in a through-space manner to the disulfide linkage; or
c. an electron initially attached to a positive site could migrate to another positive site in either a TB (along the spacer backbone) or TS (as the two "arms" approach closely enough for their Rydberg orbitals to overlap) manner. All of these processes are to be addressed in the present paper.

In the McLuckey-group paper, it was suggested that

i. the electron transfer from a positive site to the S–S bond could occur either in a through-bond or through-space manner as just mentioned; but
ii. the mechanism by which electron transfers among positive sites may occur was not discussed.

No conclusions were reached about the relative probabilities of these processes and it was not argued that the direct capture of an electron into the S–S σ* orbital to effect disulfide cleavage could be ruled out. However, it was noted that, if the only operative process were direct electron capture at the S–S σ* orbital, the variation in disulfide cleavage yield upon TMAB substitution would not be expected to be as large as observed.

As noted earlier in this Section, we already had examined the couplings and probabilities for through-bond (using methylene spacers as prototypical) electron transfer from a positive site to an S–S σ* orbital. In so doing, we characterized the magnitudes and distance dependences of the coupling matrix elements $H_{1,2}$ pertaining to this kind of process (see Fig. 4). In the present paper, we offer results in which we explore other possibilities arising from thinking about the McLuckey data.

2.3. Our models for the through-space (TS) electron transfer

In particular, we consider

1. through-space electron transfer from the ground- or excited-Rydberg orbital of a $–NH_3^+$ protonated site or from the ground- or excited-Rydberg orbital of a $–N(CH_3)_3^+$ fixed-charge site to an S–S σ* orbital; and
2. electron transfer from the ground- or excited-Rydberg orbital of one positive site (protonated or fixed-charge) to a Rydberg orbital of another positive site.

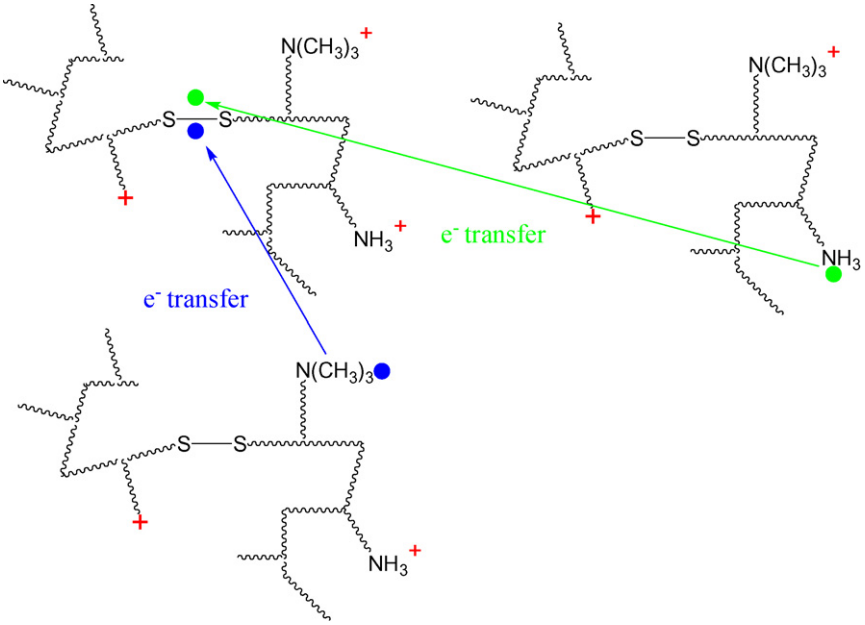

Scheme 3. Electron capture at protonated or fixed-charge site followed by migration to the disulfide bond.

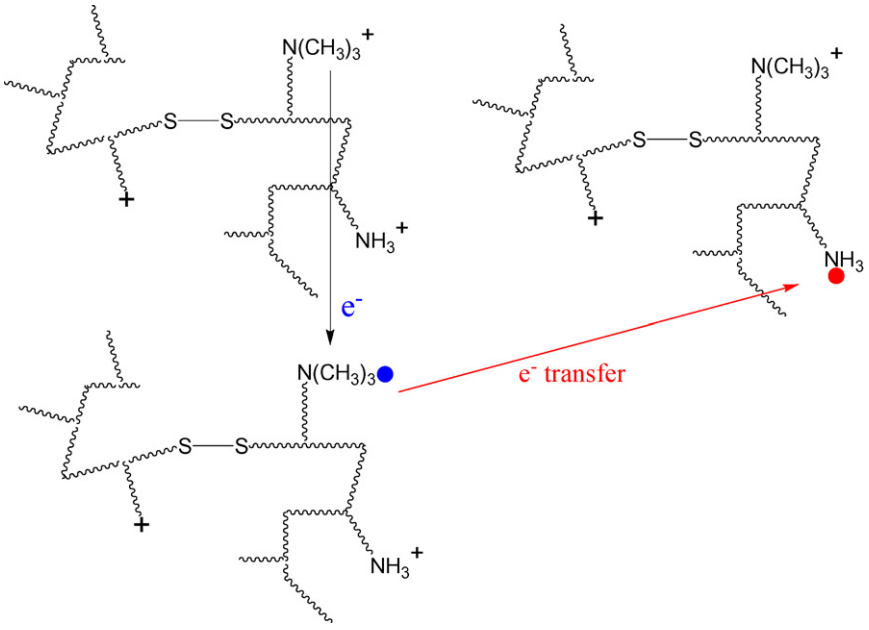

Scheme 4. Electron capture at one positive site followed by migration to another positive site.

2.3.1. Transfer from a side-chain terminus to the disulfide linkage

To model the former process, we use either an ammonium NH_4^+ or tetra-methyl ammonium $N(CH_3)_4^+$ cation to represent the protonated or fixed-charge positive site, respectively, and we use $H_3C–S–S–CH_3$ to model the disulfide linkage site. We do not connect these two units with chemical bonds because we want to explicitly exclude any contributions from through-bond processes in this set of studies (n.b., we already evaluated the TB couplings as discussed earlier and illustrated in Fig. 4). We vary the distance R_{NS} between the nitrogen atom of the positive site to the midpoint of the S–S bond and compute the energies of three electron-attached species as functions of the S–S bond length: (i) the state with an electron in the S–S σ* orbital, (ii) the state with an electron in the ground-Rydberg orbital, and (iii) the state with an electron in an excited-Rydberg orbital. We then find curve crossings between Rydberg- and σ*-attached states, from which we compute the corresponding through-space coupling matrix elements $H_{1,2}$ much as described earlier. We carry out such calculations at a range of R_{NS} distances to consider what happens as the "arms" (Lys, Ala, and Thr) undergo motions that bring them within such distances of the S–S bond.

Again, we emphasize that an essential difference between the TS and TB electron transfer events is that, in the latter, a chain of "spacer" units physically connects the positive and S–S bond sites. This connection allows the Rydberg orbitals of the positive site and the σ* orbital of the S–S bond to couple with the occupied and virtual orbitals of the spacer units. In contrast, in TB electron transfer, the couplings between the Rydberg and σ* orbitals derive from the spatial overlap of these two orbitals alone and is only operative when dynamical motions of the arms cause a side-chain terminus to contact the disulfide linkage.

2.3.2. Transfer from one side-chain terminus to another

To model the process involving electron transfer from one positive site to another, we again use NH_4^+ and $N(CH_3)_4^+$ to model the two kind of sites. We compute, as functions of the distance R_{NN} between the two nitrogen atoms, the energies of diabatic states that involve (i) an electron in the ground-Rydberg orbital of $N(CH_3)_4$ interacting with NH_4^+, (ii) an electron in an excited-Rydberg orbital of $N(CH_3)_4$ interacting with NH_4^+, (iii) an electron in the ground-Rydberg orbital of NH_4 interacting with $N(CH_3)_4^+$, and (iv) an electron in an excited-Rydberg orbital of NH_4 interacting with $N(CH_3)_4^+$. We then search for crossings of these adiabatic states to determine whether, and with what coupling strengths, near-resonant electron transfer might be expected. We carry out these calculations for various distances R_{NN} between the charged groups to simulate what happens as the terminus of one of the "arms" (Lys, Ala, Thr) that holds the attached electron undergoes motion that brings it to within various distances R_{NN} of another arm's terminus (the one to which the electron is putatively transferred). It should be emphasized that there is no Coulomb repulsion between the two side chains whose termini undergo such encounters because one of the termini has an electron attached to it.

3. Methods

Based on our earlier experience in electron transfer modeling [12], we decided to first perform our calculations at the Hartree–Fock (HF) self-consistent field (SCF) level of theory and to then extend our investigations to the unrestricted second-order Møller–Plesset (UMP2) level of theory in the next step.

The structures (bond lengths and angles) of the systems investigated $H_3C–S–S–CH_3\cdots NH_4^+$ and $H_3C–S–S–CH_3\cdots N(CH_3)_4^+$ were first partially optimized at the Hartree–Fock level with the distance between the

nitrogen atom and the midpoint of the sulfur–sulfur bond held fixed throughout the optimization calculations. Then in subsequent UMP2 calculations, we froze the geometry because we were attempting to model the environment within a peptide or protein in which an S–S σ* orbital is Coulomb stabilized by a positively charged site whose location remains quite fixed. In addition, we wanted to extract information about the distance-dependence of the electron transfer rates, so it was important to have the distance from the S–S bond to the NH_4^+ and the $N(CH_3)_4^+$ sites held fixed.

The addition of one set (1s1p) of extra-diffuse basis functions [13] centered on the nitrogen atom to the aug-cc-pVDZ basis sets [14] is necessary to properly describe the ground and excited Rydberg states of the NH_4 and $N(CH_3)_4$ species. This kind of basis was shown earlier [13] to be capable of reproducing the energies of such low-energy Rydberg states of nitrogen-centered radicals. With only four such extra diffuse functions in our basis, the number of Rydberg levels that we can describe is, of course, limited.

To evaluate the probabilities for electron transfer, we generated the necessary energy surfaces of corresponding ammonium and tetra-methyl ammonium species performing the calculations at the unrestricted second-order Møller–Plesset (UMP2) level and examining the energies of the ground-Rydberg, excited-Rydberg, and S–S σ*-attached states as functions of the S–S bond length (with the other internal coordinates of $H_3C–S–S–CH_3\cdots NH_4$ and $H_3C–S–S–CH_3\cdots N(CH_3)_4$ systems held fixed for the reasons noted earlier). The use of an unrestricted method was necessary both to achieve a qualitatively correct description of the homolytic cleavage of the S–S bond and because the various electron-attached $H_3C–S–S–CH_3\cdots NH_4$, $H_3C–S–S–CH_3\cdots N(CH_3)_4$ species are open shell systems.

Because the methods we used are based on an unrestricted Hartree–Fock starting point, it is important then to make sure that little, if any, artificial spin contamination enters into the final wave functions. We computed $\langle S^2\rangle$ for species studied in this work and found values not exceeding (after annihilation) the expected value of 0.75 by more than 0.06 in all open-shell doublet neutral cases.

Special difficulties arise when carrying out computations of not just the lowest-energy electron-attached state at each S–S bond length, but the energies of several such states. In such cases, great care must be taken to avoid variational collapse. For the ground-Rydberg state, this was not an issue, but it was for the excited-Rydberg state and for the σ*-attached state at some geometries. For the excited-Rydberg case, we found it adequate to use the "alter" option in the Gaussian program to begin the iterative SCF process with the desired orbital occupancy. Convergence to the desired (excited Rydberg) state was then verified by visually inspecting the singly occupied orbital after convergence. For the state in which the electron is attached to the S–S σ* orbital, we had to use another approach because variational collapse took place during the SCF iterations even when we used the "alter" option. In the method we used to overcome the problem for this state, we introduced a device that we have employed in many past applications [15]. Specifically, we artificially increased the nuclear charges by a small amount δq of the atoms (the sulfur atoms for the S–S σ* state) involved in accepting the transferred electron, and carried out the UMP2 calculations with these artificial nuclear charges. By plotting the energies of the states of $H_3C–S–S–CH_3\cdots NH_4$ and $H_3C–S–S–CH_3\cdots N(CH_3)_4$ for several values of the charge increment δq and extrapolating to $\delta q = 0$, we were able to evaluate the true energy of these states.

To address the issue of the electron transfer from the ground or excited Rydberg orbital of one positive site (protonated or fixed-charge) to another, we employed an approach very similar to the one described above. In this model we exploit NH_4^+ and $N(CH_3)_4^+$ to simulate the two kinds of sites.

We carried out, at the unrestricted second-order Møller–Plesset (UMP2) level, the calculations of energy profiles of the ground-Rydberg, and excited-Rydberg states of both: (i) the $NH_4\cdots N(CH_3)_4^+$ and (ii) the $NH_4^+\cdots N(CH_3)_4$ systems as functions of the NN distance, allowing partial optimization of other internal coordinates to take place. The only parameter held fixed throughout all optimization calculations was the distance between the two nitrogen atoms.

Finally, we note that all calculations were performed using the Gaussian 03 suite of programs [16], and the three-dimensional plots of the molecular orbitals were generated with the MOLDEN program [17].

4. Results

4.1. Through-space side-chain Rydberg-to-S–S σ* electron transfer

In Fig. 6a we show the energy profiles, as functions of the S–S bond length, of the ground-Rydberg state (open triangles) and excited-Rydberg state (inverted open triangles) as well as of the S–S σ*-attached state (circles). The energies of the parent cation, with no electron attached, are shown as open squares. For the σ*-attached state, profiles are displayed for five distances between the nitrogen atom and the middle of the S–S bond: R_{NS} = 15, 10, 5, 4, or 3 Å (top-through bottom curves) for $H_3C–S–S–CH_3\cdots NH_4$. In Fig. 6b, analogous curves (but only four σ*-attached curves having R_{NS} = 15, 10, 5, and 4 Å (top to bottom)) for $H_3C–S–S–CH_3\cdots N(CH_3)_4$. In these figures, the values of the coupling elements $H_{1,2}$ (cm^{-1}) determined at each avoided crossing are also specified near the avoided crossings between a Rydberg- and σ*-attached state. It should be mentioned that for $R_{NS} < 3$ Å (for the NH_4 case) and $R_{NS} < 4$ Å (for the $N(CH_3)_4$ case), steric repulsions among the other valence electrons of the disulfide and amine units cause the energies of the σ*-attached curves to increase significantly. Thus, dynamical encounters between the disulfide and amine units are not likely to access shorter R_{NS} distances than accounted for in Fig. 6, so σ* curves for such shorter distances have not been shown.

When considering the broader implications of the model-system results shown in Fig. 6a and b, is it important to think about how the energy profiles displayed in these figures will be altered by the presence of additional positive charges. After all, most ECD/ETD experiments are carried out on multiply

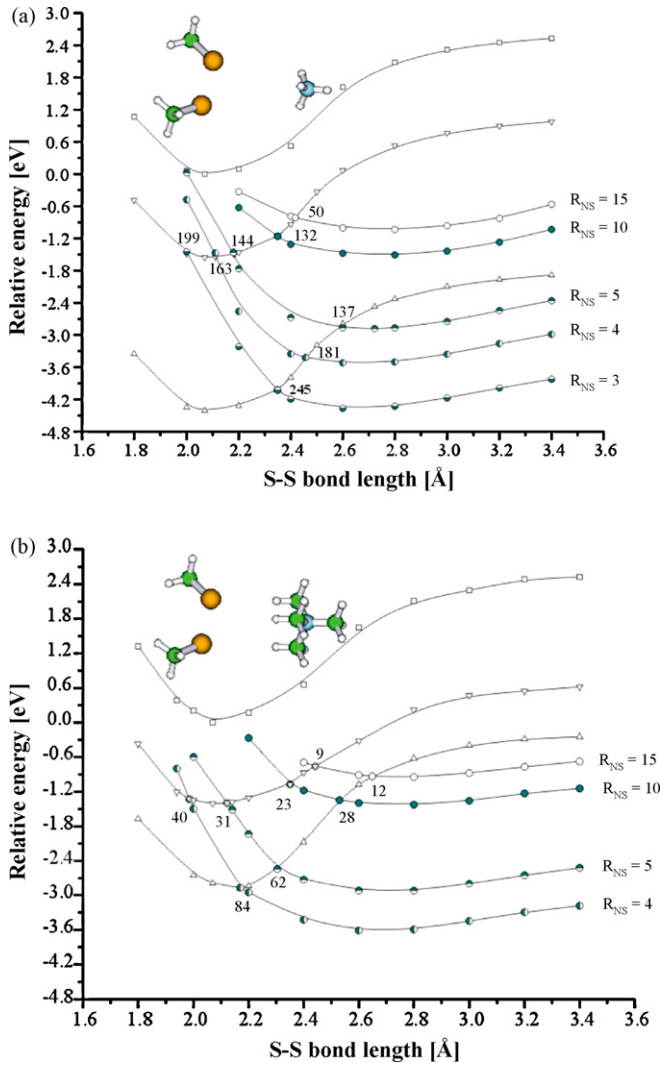

Fig. 6. Energy profiles for ground-Rydberg (triangles), excited-Rydberg (inverted triangles), and σ*-attached states (circles) for $H_3C–S–S–CH_3\cdots NH_4$ (a) and $H_3C–S–S–CH_3\cdots N(CH_3)_4$ (b) as functions of S–S bond length. Also shown (squares) is the energy of the parent $H_3C–S–S–CH_3\cdots NH_4^+$ cation (open squares). The values of R_{NS} at which σ*-attached states' energies are displayed are shown on the right of each figure.

charged cations. The largest effect of additional positive charge will be to lower all of the electron-attached surfaces relative to the parent cation's surface by an amount that depends on the additional Coulomb stabilization provided by the additional positive charges. However, the more important (to electron transfer) effects arise when additional positive charges modify the relative positions of the electron-attached states. The relative energies of the Rydberg-attached and σ*-attached surfaces will be altered by amounts that depend on the differences in Coulomb stabilization generated by the additional positive charges. For example, a second positive charge located closer to the S–S bond than to the Rydberg site will differentially stabilize the σ*-attached state and thus move the intersection point for the Rydberg- and σ*-attached curves to smaller *R* and lower energy. Positive charges closer to the Rydberg site than to the S–S bond will have the opposite effect.

Some important observations about the data displayed in Fig. 6 and conclusions drawn from these observations can now be made.

i. *For the protonated-site model* NH_4, within the range of S–S bond lengths (i.e., 2.1 ± 0.1 Å) that are thermally accessible under vibrational motion at temperatures common in ECD or ETD, the excited-Rydberg state is crossed by the σ*-attached state for R_{NS} distances between 3 Å and 5 Å. The ground-Rydberg state is crossed by the σ*-attached state only if the S–S vibration is substantially excited or if other positive charges are present and closer to the S–S bond than to the Rydberg site and thus shift the σ*-attached state to lower energy [18]. So, it appears that electron transfer from either the ground- or an excited-Rydberg state to the S–S σ* state can be expected to occur, especially for multiply positively charged species. However, there are processes that compete against such TS electron transfer events. In particular, TS transfer from any excited Rydberg state would have to occur during a time interval of a few μs (the radiative and radiationless relaxation times of excited-Rydberg states have been found to be in this range [19]) after capture of an electron at the protonated site. Moreover, once the excited-Rydberg state has decayed to the ground-Rydberg state, hydrogen atom loss occurs [20] within ca. 10^{-12} s. So, TS electron transfer from the ground Rydberg state to the S–S bond is even less likely because it can occur only within this very short 10^{-12} s time window. TS transfer from an excited Rydberg state to the S–S bond is more likely because it has a 10^{-6} s window of opportunity.

ii. The ground-Rydberg state of the *fixed-charge model* $N(CH_3)_4$ is crossed by the σ*-attached state for R_{NS} values near 4 Å (probably ± 0.5 Å). For significantly longer R_{NS} distances, the crossing with the ground-Rydberg state occurs at longer S–S bond lengths. So either vibrational excitation or differential Coulomb stabilization of the σ* orbital by other positive sites would be needed to effect TS transfer from the ground Rydberg state. The σ*-attached state crosses the excited-Rydberg state at S–S bond lengths between 2.0 Å and 2.2 Å for R_{NS} between 4 Å and 5 Å. However, again there are competing processes to consider. Any TS electron transfer from an excited Rydberg state would have to occur within a window of ca. 10^{-6} s, the combined radiative and radiationless relaxation time of such states. Although the ground-Rydberg state of the fixed-charge species is not subject to H atom loss, such species have been found [21] to undergo N–C bond cleavage at rates of ca. 10^6 s^{-1}. So, for the fixed-charge species, both the excited- and ground-Rydberg states have windows of opportunity in the 10^{-6} s range to produce TS electron transfer.

So, it appears that TS transfer from excited Rydberg states of protonated species and from ground- or excited-Rydberg states of fixed-charge species can occur, but only over a time window of ca. 10^{-6} s after electron capture at the positive site. Of course, in addition, the rate of such transfer events will depend upon both the frequency $\nu_{contact}$ with which the charged site encounters the

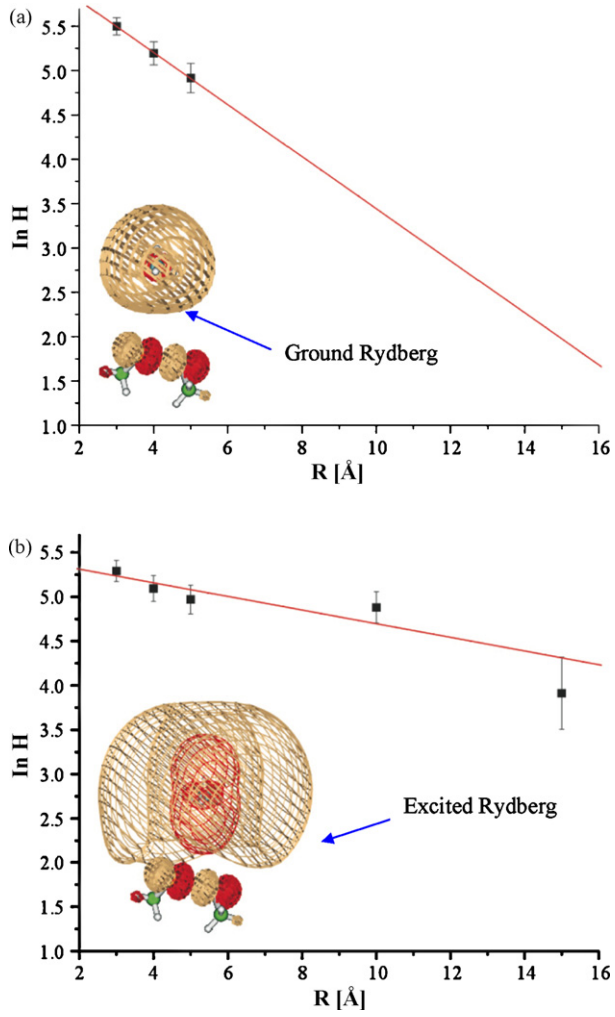

Fig. 7. $H_{1,2}$ couplings (cm^{-1}) between ground- (a) and excited- (b) Rydberg orbitals of NH_4 and the S–S σ* orbital as functions of the distance R_{NS} (Å) between the nitrogen atom and the midpoint of the S–S bond.

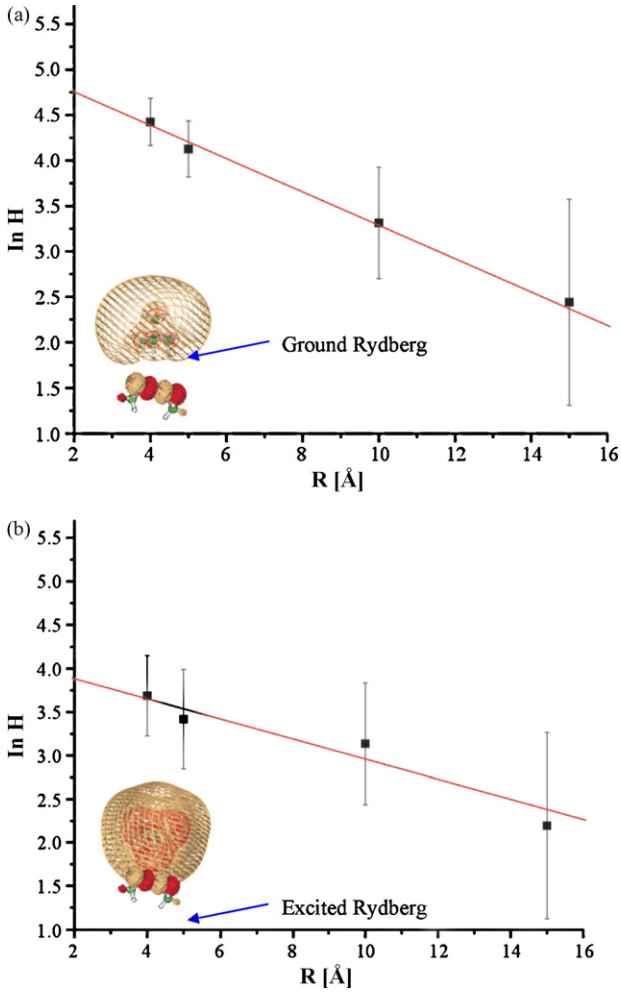

Fig. 8. $H_{1,2}$ couplings (cm^{-1}) between ground- (a) and excited- (b) Rydberg orbitals of $N(CH_3)_4$ and the S–S σ* orbital as functions of the distance R_{NS} (Å) between the nitrogen atom and the midpoint of the S–S bond.

S–S σ* orbital and the strength $H_{1,2}$ of the orbital coupling (i.e., the 84 cm^{-1} in Fig. 6b). It is to these $H_{1,2}$ couplings that we now turn our attention.

In Fig. 7a, we show the TS electron transfer coupling matrix elements $H_{1,2}$ for the process in which an electron migrates from the ground-Rydberg orbital of NH_4 to the S–S σ* orbital as functions of the distance R_{NS} from the nitrogen atom to the middle of the S–S bond. Fig. 7b shows the corresponding data for the ($n=4$) excited-Rydberg orbital of NH_4. Fig. 8a and b shows the $H_{1,2}$ matrix elements for the transfer of an electron from the corresponding ground- and excited-Rydberg orbitals of $N(CH_3)_4$ to the S–S σ* orbital. As we have done in past work, error bars corresponding to ±50 cm^{-1} uncertainty in the $H_{1,2}$ values are also shown.

Again, we see that the $H_{1,2}$ couplings fall off exponentially with distance, as expected, and we note that the $H_{1,2}$ couplings found for these through-space electron transfers are similar in magnitude to those we found earlier for through-bond transfer (over five or fewer bonds). So, the Landau–Zener estimates of the surface-hopping probabilities (p) for through-space and through-bond electron transfer should be of similar magnitudes. Therefore, the rate of through-space electron transfer, evaluated by multiplying the surface-hopping probability p by the frequency $\nu_{contact}$ with which a positive site encounters the S–S bond and the probability P that the S–S bond can access the crossing point, will be much smaller than the rates of through-bond transfer (see Eq. (1)) because $\nu_{SS} \gg \nu_{contact}$.

Let us summarize our most important findings in terms of interpreting the kind of data reported by the McLuckey group. First, (Fig. 8) the $H_{1,2}$ coupling elements are somewhat larger for the protonated (NH_4) species than for the fixed-charge species ($N(CH_3)_4$). The ground- and excited-Rydberg states of fixed-charge species should be capable of inducing TS electron transfer, but only during a ca. 10^{-6} s time window. The excited-Rydberg states of protonated species can also induce TS electron transfer over a similar time window, but the ground-Rydberg state of the protonated species is less likely to induce TS transfer because it undergoes H atom loss in ca. 10^{-12} s.

The probability p for a TS electron transfer from a fixed-charge site to the S–S σ* orbital can be estimated using

LZ theory:

$$p = 2\exp\left[\frac{-2\pi H_{1,2}^2}{\hbar v \delta F}\right]\left(1-\exp\left[\frac{-2\pi H_{1,2}^2}{\hbar v \delta F}\right]\right). \quad (2)$$

Here, v is the speed with which the R_{SS} coordinate moves through the curve crossing, $H_{1,2}$ is the coupling matrix element (ca. 84 cm^{-1} from Fig. 6b for R_{NS} = 4 Å), and δF is the difference is slopes of the ground-Rydberg and σ*-attached curves at the crossing. We note that this evaluation of p proceeds in exactly the same manner for TS as for TB electron transfer. As a result, the surface-hopping probabilities for the TS and TB processes are expected to be very similar for a given value of $H_{1,2}$. In our earlier work on TB transfer in H_3C–S–S–$(CH_2)_n$–NH_3 models, the $H_{1,2}$ elements ranged from 800 cm^{-1} (for n = 1) to 70 cm^{-1} (for n = 3), and the resulting hopping probabilities ranged from 0.6 (for n = 1) to 0.05 (for n = 3). The 84 cm^{-1} $H_{1,2}$ value found for the ground-Rydberg state of the fixed-charge species at R_{NS} = 4 Å would produce a probability of ca. 0.08 for the TS electron transfer process.

The rate (events per second) of TS electron transfer is computed by multiplying p by the frequency $\nu_{contact}$ with which the fixed-charge and S–S bond sites come within 4 Å of one another. As explained earlier, the rate of TB transfer is computed by multiplying the p by the frequency ν_{SS} of vibration of the S–S bond (assuming one is dealing with a crossing that is thermally accessible). Because ν_{SS} is expected to be considerably larger than the frequency $\nu_{contact}$, the rates of TB transfer are predicted to substantially exceed those of TS transfer. However, the TB rates decay very quickly with the distance between the disulfide and charged sites as shown in Fig. 4 (e.g., they can probably be ignored after a distance of 5 or 6 bonds). So, TB transfer is probably only feasible over distances of 10–15 Å. TS transfer between a disulfide site and a side-chain terminus separated by substantially more bonds can occur (albeit at a rate limited by $\nu_{contact}$) if these sites come within ca. 4–10 Å through folding movement of the side chain(s) and attach an electron while residing at such distances (because they have only ca. 10^{-6} s to effect TS transfer).

4.2. Electron transfer from one positive site to another

In Fig. 9 we show, as functions of the distance R_{NN} between the two nitrogen atoms, the energies of states that involve (i) an electron in the ground-Rydberg orbital of $N(CH_3)_4$ interacting with NH_4^+, (ii) an electron in an excited-Rydberg orbital of $N(CH_3)_4$ interacting with NH_4^+, (iii) an electron in the ground-Rydberg orbital of NH_4 interacting with $N(CH_3)_4^+$, and (iv) an electron in an excited-Rydberg orbital of NH_4 interacting with $N(CH_3)_4^+$. These data are central to addressing whether, and at what rate, electron transfer can occur between protonated and fixed-charge termini.

These data show that there are no curve crossings connecting a state with the electron on one of the charged sites to a state with the electron on the other site. This means that resonant (and thus facile) TS electron transfer will probably not occur between protonated and fixed-charge sites. The mechanism by with electron transfer might occur between these sites involves a radiationless transition much like what occurs when electronically excited-Rydberg states relax to lower-energy Rydberg states by converting electronic energy into internal vibrational energy. However, the radiationless transitions for our $[NH_4\cdots N(CH_3)_4]^+$ species would have to occur within the brief time window during which the two sites' Rydberg orbitals are within contact of one another (i.e., with 2 Å < R_{NN} < 14 Å as can be inferred from Fig. 9).

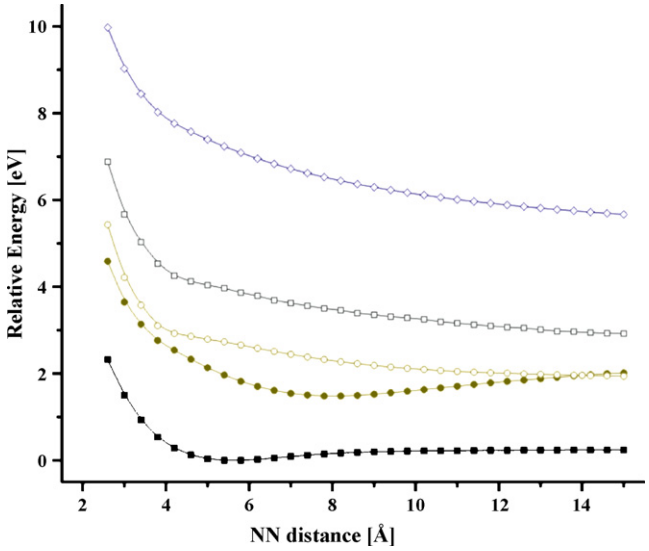

Fig. 9. Energies of $NH_4^+\cdots N(CH_3)_4^+$ (open diamonds); ground- (filled squares) and excited- (open circles) $NH_4\cdots N(CH_3)_4^+$ Rydberg states with electron attached to protonated site; ground- (filled circles) and excited- (open squares) $NH_4^+\cdots N(CH_3)_4$ Rydberg states with electron attached to fixed-charge site as functions of the distance between the two nitrogen atoms.

We know that radiationless relaxation of the individual NH_4 and $N(CH_3)_4$ species' excited-Rydberg states occurs on μs timescales, so at rates in the 10^6 s^{-1} range. The small geometry differences among various Rydberg states produce Franck–Condon like factors that do not generate much vibrational energy change, thus producing such slow rate of relaxation. Although the higher density of vibrational states available within the $[NH_4\cdots N(CH_3)_4]^+$ complex might increase this rate an order of magnitude or two, it is unlikely that the rate would exceed 10^8 s^{-1} for our $[NH_4\cdots N(CH_3)_4]^+$. Fig. 9 shows that the range over which the two Rydberg orbitals in $[NH_4\cdots N(CH_3)_4]^+$ interact substantially (i.e., where the potential curves are not flat) is ca. 12 Å. An encounter between two side-chain termini (one neutral and one positively charged) induced by thermal motion at room temperature or somewhat above would likely traverse 12 Å in a time far shorter than 10^{-8} s in these gas-phase samples. This leads us to predict that radiationless relaxation in $[NH_4\cdots N(CH_3)_4]^+$ will not occur within the duration of a collision between two unlike termini and thus that TS electron transfer between protonated and fixed-charge termini is likely to be very slow.

In contrast to these slow rates for electron transfer between protonated and fixed-charge sites, electron transfer from one protonated site to another or from one fixed-charge site to another should be quite facile because little or no electronic energy need

be gained or lost in such processes. The limiting factor governing the rate of electron transfer between sites of like electron-binding character would be the rates at which the sites come within ca. 10 Å (the distance at which Fig. 9 shows the Rydberg orbitals to begin to interact significantly).

5. Summary

5.1. Findings

The primary findings and predictions of our study are as follows:

1. Electron transfer between protonated and fixed-charge side-chain termini is slow, but transfer from protonated to protonated or from fixed-charge to fixed-charge sites should be facile with rates governed by the encounter frequencies of pairs of such sites.
2. Through-bond electron transfer from a protonated or fixed-charge terminus to an S–S σ* orbital can occur over ca. 15 Å, covering ca. five intervening bonds, with probabilities of 10^{-3} to 10^{-1} per vibration of the S–S bond. Thus, the rates can be 10^{10} to 10^{12} s^{-1} because the S–S bond vibrates at a frequency (ν_{SS}) near 10^{13} s^{-1}.
3. Through-space electron transfer from a protonated terminus to an S–S bond may be slow unless the S–S bond is stretched or additional positively charged sites act to differentially stabilize the σ*-attached site. Excited-Rydberg states have a window of opportunity of ca. 10^{-6} s after electron attachment to effect TS electron transfer. The ground-Rydberg state has only ca. 10^{-12} to effect transfer.
4. Through-space electron transfer from the ground- or excited-Rydberg state of a fixed-charge terminus to an S–S bond can occur but only within a time window of ca. 10^{-6} s after electron attachment.
5. The probabilities of such TS transfer can be high (e.g., 0.1 per contact between the S–S bond and the terminus), but the rates will be limited by the very brief windows of opportunity available.
6. Because the contact frequency $\nu_{contact}$ for a protonated or fixed-charge terminus encountering a S–S bond is likely much smaller than the vibrational frequency ν_{SS} of the S–S bond, the rates of TS electron transfer are expected to be lower than rates of TB electron transfer when the latter are operative (i.e., through ca. 5 bonds or 15 Å).

5.2. Applications to model peptides in Figs. 1 and 5

What can we say from these conclusions about the ECD/ETD data on the compounds shown in Figs. 1 and 5? For the helical polypeptide shown in Fig. 1:

a. Our earlier results suggest that electron attachment to either of the two positively charged Lys termini occurs 10–100 times as often as does direct attachment to the Coulomb-stabilized S–S σ* orbital.
b. However, TB electron transfer from a Lys terminus to the S–S bond is unlikely; there are just too many intervening bonds to migrate through.
c. TS electron transfer from a Lys terminus to the S–S bond is also unlikely; the helical backbone is too rigid and the Lys side chain too short to allow the Lys and S–S sites to come within the requisite ca. 4 Å.
d. Hence, although only 1–10% of the electron attachment occurs via Coulomb-stabilized direct attachment to the S–S σ* orbital, this is the dominant pathway for disulfide cleavage for this compound.
e. It is possible that TB or TS electron transfer from a Lys terminus to the π* orbitals of the Ala amino acids closest to this terminus can induce backbone cleavage at these sites. However, it is also possible the Coulomb-stabilized direct attachment to Ala amide π* orbitals close to these termini cause such cleavage. Certainly, the range over which N–C_α cleavage is observed is consistent with what the Coulomb stabilization model would predict.
f. Because the disulfide linkage is spatially "exposed" (i.e., not subject to severe steric hindrance), ETD should be able to cause disulfide cleavage much as was found in the ECD experiments, so we recommend that such ETD experiments be carried out.

For the more flexible polypeptides shown in Fig. 5 having a disulfide-linked core from which "arms" extend:

a. Again, we expect that most of the initial electron attachment occurs at a side chain's positive termini (protonated or fixed-charge).
b. However, a few percent of the initial attachment events might occur directly to the S–S σ* orbital generating prompt disulfide cleavage. Because the McLuckey group experiments on these peptides were performed using ETD (with the electron transfer agent being azobenzene anion) rather than ECD, it is possible that steric hindrance may have precluded the anion reaching the S–S bond site thus further reducing the S–S σ* attachment yield. Therefore, it would be wise to study these compounds under ECD conditions to see whether enhanced S–S cleavage occurs due to the free electrons' enhanced ability to access the Coulomb-stabilized S–S σ* orbital.
c. TB electron transfer from a side chain's terminus to the S–S bond is unlikely; there are too many (between 9 and 15 for the protonated species and between 14 and 20 for the fully TMAB-substituted species) intervening bonds.
d. TS electron transfer from a fixed-charge side chain's terminus to the S–S bond can occur, as can TS electron transfer from a protonated side chain's terminus, but the latter is expected to be less probable because its ground-Rydberg state is inactivated within ca. 10^{-12} s by H atom loss. The rates of both processes will be limited by the frequencies with which the termini come within contact distance of the S–S bond.
e. TS electron transfer between protonated and fixed-charge side-chain termini cannot easily occur, but TS electron transfer from protonated to protonated or from fixed-charge to

Table 1
Number of intervening bonds, average and maximum distances from side-chain terminus to disulfide linkage

Protonated	Number of bonds	Average distance (Å)	Maximum distance (Å)
Ala	9	5.0	10
Lys	10	8.8	12
Thr	15	6.2	19
Fixed-charge			
Ala	14	5.4	16
Lys	15	12	18
Thr	20	10	25

fixed-charge is facile (if the two termini come within a few Å).

5.3. Physical pictures of how disulfide cleavage occurs

5.3.1. The rigid, extended, helical peptide

In summary, for the more rigid helical structure shown in Fig. 1, our findings suggest that the only feasible mechanism for disulfide cleavage is through Coulomb-stabilized direct attachment to the S–S σ* orbital. The fact that limited N–C_α backbone cleavage (i.e., for amino acids within ca. 6 Å of the positive termini) was also observed is also consistent with this direct-attachment (to amide π* orbitals) mechanism. Again, it should be emphasized that electron attachment (in ECD or transfer in ETD) probably occurs mainly at the positively charged termini, but, for this model system, only the fraction of electron attachment events taking place at the S–S bond site can generate disulfide cleavage.

5.3.2. The flexible, crowded peptides

When analyzing the more flexible structures shown in Fig. 5, it is important to first consider the differences among the distances and number of intervening bonds between the disulfide linkage and the termini of the three "arms" holding the positive charges. The number of intervening bonds will influence the TB electron transfer probabilities and the distances will influence the TS probabilities. In Table 1, we list these distances and bond numbers for the two compounds shown in Fig. 5. The maximum distances correspond to those that can be obtained by altering bond angles, but not bond lengths, along the backbone, and the average distance is that characterizing the thermal equilibrium structure.

The primary thing to notice in this data is that, for both protonated and fixed-charge species, the Ala "arm" is considerably closer to the disulfide linkage than the other two arms. Moreover, it resides [22] within the range of distances (see Fig. 6) within which TS electron transfer can be expected. This difference plays a role in our postulating a model, based on the findings of the present paper, for the McLuckey group's observations about S–S cleavage patterns.

A striking finding reported in Ref. [4] is that the compounds in which all but one of the charge sites involved fixed charges produce unusually low fractions of S–S bond cleavage. For example, for compounds as in Fig. 5, those with three protonated sites had 71% of their cleavages being S–S cleavage, those with two protonated sites had 68%, those with one protonated site had only 36%, and those with no protonated (i.e., all fixed-charge) sites had 80%. In addition, the total fractions of events that produced any cleavage (S–S, or backbone, or side-chain loss) were, respectively, 83, 82, 52, and 68, again displaying an anomaly for the species containing only one protonated site. With these puzzling patterns in mind and based upon the findings we report here, we now discuss what we think happens for the kind of species studied in Ref. [4].

First, as with the species shown in Fig. 1, those shown in Fig. 5 are expected to undergo electron attachment primarily at their positive termini. For the kind of species shown in Fig. 5, we expect even more limited direct electron transfer (in ETD) to the S–S σ* orbital than for the compound in Fig. 1 because of steric crowding [23] between the azobenzene anion and the surrounding backbone and side chains. However, whatever σ* attachment does occur will give rise to prompt disulfide cleavage. As noted earlier, it would be informative to repeat the experiments on these peptides using ECD rather than ETD to see whether the yield of S–S cleavage is altered (i.e., because a free electron should better be able to access the disulfide bond site).

For the (probably vast) majority of electron attachment events that take place at the positive termini, our best thoughts about what happens are as follows:

a. An electron attaches to one of the positive sites, thus reducing the charge by one unit. We do not know what the relative cross-sections for attachment to protonated and fixed-charge sites are, but we expect the former to be somewhat larger because of the higher exothermicity (ca. 4 eV at protonated sites vs. ca. 2.5 eV at fixed-charge sites) for the former. At this time and in the absence of further evidence, we will assume that capture at any positive site is possible and with similar probability.
b. For the species in Fig. 5a having three protonated sites, the attached electron can migrate (as our findings suggest) from protonated site to protonated site as the termini of these sites come into contact distance of one another. The rates of such migrations we will denote r_1. Once the electron ends up on the Ala site, which is the one closest (5 Å) to the S–S bond, it can undergo prompt (at a rate $r_2 > r_1$) TS electron transfer to the S–S σ* orbital thus giving disulfide cleavage. Electron transfer directly from one of the more distant sites to the S–S σ* orbital can also take place but at slower rates (at a rate $r_3 < r_1 < r_2$) because of the larger distances [24]. However, all of this action must occur within a window of a few μs after electron attachment because, once the excited-Rydberg states relax to the ground-Rydberg state, H atom loss occurs.
c. We now observe that, when the Ala site is TMAB-substituted, the average distance of its terminus to the S–S bond is only slightly increased compared to when it is protonated (see Table 1). Thus for the species containing zero, one, two, or three TMAB substitutions, the Ala site's terminus (substituted or not) resides, on average, ca. 5 Å from the S–S bond. We thus refer to the Ala terminus at the "close site".

d. Because adding the TMAB substitution to the Ala site makes little change in the internal Coulomb repulsion energy of the triply charged peptide, we postulate (n.b., as noted earlier, the synthetic route for this substitution is not known to guarantee this) that the first and second TMAB substitutions occur at the Lys and Thr sites. Adding TMAB to either of these sites substantially increases the average arm length (see Table 1) and thus substantially decreases the Coulomb repulsions within the peptide, thus making the products of TMAB substitution more thermodynamically stable. This postulate means that in the triply, doubly, and singly protonated species, the Ala site remains protonated; only when all three sites have been TMAB-substituted is the Ala site converted to fixed charge.
e. Based on this postulate, we then suggest that for the species having *two protonated sites* and one fixed-charge site, the electron attaches to either the close (protonated Ala) site after which it can then undergo TS transfer (at r_2) to the S–S bond, or it attaches to the Lys or Thr. An electron attached to whichever of Lys and Thr is protonated can subsequently transfer to the Ala site (at r_1) and then transfer onward (at r_2) to the S–S bond. However, any electron attached to whichever of Lys or Thr has fixed-charge character, cannot transfer to Ala. Its only way to transfer (at a rate r_4 even less than r_3 because the TMAB-substituted arm is longer) to the S–S bond is to wait until its terminus comes within contact distance (ca. 4 Å) of the S–S bond. Thus, these species are expected to have somewhat reduced disulfide cleavage rates than the fully protonated species because transfer from a distant terminus (r_4) directly to the S–S bond is slower [24] than either transfer from the close Ala (r_2) or from a distant protonated terminus (r_3) to Ala and subsequently from Ala to the S–S bond (at r_2).
f. For the species having *one protonated site* (by assumption, Ala) and two fixed-charge sites (Lys and Thr), the electron attaches to either the close (Ala) after which it can undergo TS transfer to the S–S bond (at r_2), or it attaches to the Lys or Thr. An electron attached to the Lys and Thr cannot subsequently transfer to the Ala site. Its only way to transfer to the S–S bond is to wait until its terminus comes (at rate r_4) within contact distance (ca. 4 Å) of this bond [24]. These species are thus expected to have even slower disulfide cleavage rates [25] and to have the slowest rates among all species.
g. For the species with *no protonated sites*, the attached electron can migrate from site to site (at a rate somewhat less than r_1 because of the longer arms) as the termini come into contact distance of one another. Once it ends up on the Ala site, which is the one closest (5 Å) to the S–S bond, it can undergo TS electron transfer (at a rate similar to r_2) to the S–S σ* orbital thus giving disulfide cleavage. Moreover, because the species with no protonated sites do not undergo H atom loss, they have more time for their "arms" to encounter the S–S bond. These species are thus expected to have higher disulfide cleavage rates than the species with the Ala protonated.

In summary, by assuming that (i) the Ala site is the last to be TMAB-substituted and (ii) TS transfer (r_1) among sites of similar character (i.e., protonated or fixed-charge) is facile but is not among sites of different character, (iii) TS transfer rates ($r_2 > r_3 > r_4$) from a terminus to the S–S bond depend (probably as the inverse square) upon distance, we can rationalize the primary findings from the McLuckey group's experiments. In particular, the surprising result that the compound having only one protonated site gives the least S–S cleavage can be rationalized.

Needless to say, the interpretation offered above is based on assumptions that need to be tested. It would be especially helpful if other model compounds containing protonated and/or fixed-charge sites in which the character of each site is known could be studied by ETD (and ECD for comparison) to determine the fraction of disulfide, N–C_α, and side-chain cleavage. It would also be useful to vary the degree of folding flexibility in some of the "arms" included in such studies. Such studies would offer even more data to test the predictions made in the current paper regarding how electrons can migrate TB or TS among charged sites and from charged sites to S–S σ* orbitals.

Acknowledgements

Support of the National Science Foundation through grant CHE 0500579 is appreciated. Significant computer time was provided by the Center for High Performance Computing at the University of Utah. We thank Prof. Scott McLuckey for conveying his results to us prior to their appearing in publication.

References

[1] (a) R.A. Zubarev, N.L. Kelleher, F.W. McLafferty, J. Am. Chem. Soc. 120 (1998) 3265;
(b) R.A. Zubarev, N.A. Kruger, E.K. Fridriksson, M.A. Lewis, D.M. Horn, B.K. Carpenter, F.W. McLafferty, J. Am. Chem. Soc. 121 (1999) 2857;
(c) R.A. Zubarev, D.M. Horn, E.K. Fridriksson, N.L. Kelleher, N.A. Kruger, M.A. Lewis, B.K. Carpenter, F.W. McLafferty, Anal. Chem. 72 (2000) 563;
(d) R.A. Zubarev, K.F. Haselmann, B. Budnik, F. Kjeldsen, F. Jensen, Eur. J. Mass Spectrom. 8 (2002) 337.
[2] (a) J.E.P. Syka, J.J. Coon, M.J. Schroeder, J. Shabanowitz, D.F. Hunt, Proc. Natl. Acad. Sci. 101 (2004) 9523;
(b) J.J. Coon, J.E.P. Syka, J.C. Schwartz, J. Shabanowitz, D.F. Hunt, Int. J. Mass Spectrom. 236 (2004) 33;
(c) S.J. Pitteri, P.A. Chrisman, S.A. McLuckey, Anal. Chem. 77 (2005) 5662;
(d) H.P. Gunawardena, M. He, P.A. Chrisman, S.J. Pitteri, J.M. Hogan, B.D.M. Hodges, S.A. McLuckey, J. Am. Chem. Soc. 127 (2005) 12627.
[3] (a) E.A. Syrstad, F. Turecek, J. Phys. Chem. A105 (2001) 11144;
(b) F. Turecek, M. Polasek, A. Frank, M. Sadilek, J. Am. Chem. Soc. 122 (2000) 2361;
(c) E.A. Syrstad, D.D. Stephens, F. Turecek, J. Phys. Chem. A107 (2003) 115;
(d) F. Turecek, J. Am. Chem. Soc. 125 (2003) 5954;
(e) E.A. Syrstad, F. Turecek, Am. Soc. Mass Spectrom. 16 (2005) 208;
(f) E. Uggerud, Int. J. Mass Spectrom. 234 (2004) 45;
(g) I. Anusiewicz, J. Berdys-Kochanska, J. Simons, J. Phys. Chem. A109 (2005) 5801;
(h) I. Anusiewicz, J. Berdys-Kochanska, P. Skurski, J. Simons, J. Phys. Chem. A110 (2006) 1261;
(i) A. Sawicka, P. Skurski, R.R. Hudgins, J. Simons, J. Phys. Chem. B107 (2003) 13505;
(j) M. Sobczyk, P. Skurski, J. Simons, Adv. Quantum Chem. 48 (2005) 239;
(k) A. Sawicka, J. Berdys-Kochaska, P. Skurski, J. Simons, Int. J. Quantum Chem. 102 (2005) 838;

(l) I. Anusiewicz, J. Berdys, M. Sobczyk, A. Sawicka, P. Skurski, J. Simons, J. Phys. Chem. A109 (2005) 250;
(m) V. Bakken, T. Helgaker, E. Uggerud, Eur. J. Mass Spectrom. 10 (2004) 625;
(n) P. Skurski, M. Sobczyk, J. Jakowski, J. Simons, Int. J. Mass Spectrom. 265 (2007) 197.

[4] H.P. Gunawardena, L. Gorenstein, D.E. Erickson, Y. Xia, S.A. McLuckey, Int. J. Mass Spectrom. 265 (2007) 130.

[5] C. Dezarnaud-Dandine, F. Bournel, M. Troncy, D. Jones, A. Modelli, J. Phys. B: At. Mol. Opt. Phys. 31 (1998) L497;
M. Seydou, A. Modelli, B. Lucas, K. Konate, C. Desfrancois, J.P. Schermann, Eur. Phys. J. D 35 (2005) 199.

[6] R. Hudgins, K. Håkansson, J.P. Quinn, C.L. Hendrickson, A.G. Marshall, Proceedings of the 50th ASMS Conference on Mass Spectrometry and Allied Topics, Orlando, Florida, June 2–6, 2002, p. A020420, Fig. 1 first appears in publication in Ref. [3i].

[7] (a) The workers of Ref. [3i] cite the following reference in support of this claim: R.R. Hudgins, M.F. Jarrold, J. Am. Chem. Soc. 121 (1999) 3494, In this paper, a singly-charged analog of the species shown in Fig. 1 was used and found to display extended rather than compact structure, suggesting that the doubly-charged species would also be extended because it would also have internal Coulomb repulsion between the two positive Lys sites;
(b) A more recent effort aimed at using mobility measurements to probe extended and more compact structures of alanine-containing peptides is given in A.E. Counterman, D.E. Clemmer, J. Phys. Chem. B 107 (2003) 2111.

[8] (a) M. Sobczyk, J. Simons, J. Phys. Chem. B 110 (2006) 7519;
(b) M. Sobczyk, J. Simons, Int. J. Mass Spectrom. 253 (2006) 274.

[9] In this study, the lowest excited Rydberg state of one higher principal quantum number was studied. For $–NH_3$ Rydberg radicals, the ground-Rydberg state is labeled with $n = 3$ principal quantum number because the nitrogen 1s and four bonding electron pairs occupy 1s, 2s, and 2p orbitals in the united-atom limit, so the Rydberg electron resides in an $n = 3$ orbital. So, the excited Rydberg orbital shown has $n = 4$.

[10] The geometries shown in Fig. 5 represent those of the minimum-energy structures found using a PM3 force field.

[11] In a future work, we will examine transfer from positive sites to amide π^* orbitals, but, for the present paper, we restrict our attention to transfer to disulfide σ^* orbitals. The amide π^* orbitals can play roles in effecting N–C_α cleavage.

[12] See Refs. [8a] and [8b] as well as Ref. [3h].

[13] (a) M. Gutowski, J. Simons, J. Chem. Phys. 93 (1990) 3874;
(b) P. Skurski, M. Gutowski, J. Simons, Int. J. Quantum Chem. 80 (2000) 1024.

[14] R.A. Kendall, T.H. Dunning Jr., R.J. Harrison, J. Chem. Phys. 96 (1992) 6796.

[15] See Ref. [3l]. This device was first used in B. Nestmann, S.D. Peyerimhoff, J. Phys. B 18 (1985) 615;
See Ref. [3l]. This device was first used in B. Nestmann, S.D. Peyerimhoff, J. Phys. B 18 (1985) 4309.

[16] M.J. Frisch, G.W. Trucks, H.B. Schlegel, G.E. Scuseria, M.A. Robb, J.R. Cheeseman, J.A. Montgomery, Jr., T. Vreven, K.N. Kudin, J.C. Burant, J.M. Millam, S.S. Iyengar, J. Tomasi, V. Barone, B. Mennucci, M. Cossi, G. Scalmani, N. Rega, G.A. Petersson, H. Nakatsuji, M. Hada, M. Ehara, K. Toyota, R. Fukuda, J. Hasegawa, M. Ishida, T. Nakajima, Y. Honda, O. Kitao, H. Nakai, M. Klene, X. Li, J.E. Knox, H.P. Hratchian, J.B. Cross, C. Adamo, J. Jaramillo, R. Gomperts, R.E. Stratmann, O. Yazyev, A.J. Austin, R. Cammi, C. Pomelli, J.W. Ochterski, P.Y. Ayala, K. Morokuma, G.A. Voth, P. Salvador, J.J. Dannenberg, V.G. Zakrzewski, S. Dapprich, A.D. Daniels, M.C. Strain, O. Farkas, D.K. Malick, A.D. Rabuck, K. Raghavachari, J.B. Foresman, J.V. Ortiz, Q. Cui, A.G. Baboul, S. Clifford, J. Cioslowski, B.B. Stefanov, G. Liu, A. Liashenko, P. Piskorz, I. Komaromi, R.L. Martin, D.J. Fox, T. Keith, M.A. Al-Laham, C.Y. Peng, A. Nanayakkara, M. Challacombe, P.M.W. Gill, B. Johnson, W. Chen, M.W. Wong, C. Gonzalez, J.A. Pople, Gaussian, Inc., Wallingford CT, 2004.

[17] G. Schaftenaar, J.H. Noordik, J. Comput. Aided Mol. Des. 14 (2000) 123.

[18] As remarked earlier, for the species studied in the experiments, there are more than two positive charges present. Thus, it is possible that another positive charge may be closer to the S–S bond than to the positive site holding the attached electron and thus may energy-stabilize the S–S σ^* curve more than the Rydberg curve. This would then cause the crossing of the σ^* and ground-Rydberg curves to occur within the thermally accessible region.

[19] See Ref. [3e] as well as F. Turecek, P.J. Reid, Int. J. Mass Spectrom. 222 (2003) 49.

[20] F. Turecek, E.A. Syrstad, J. Am. Chem. Soc. 125 (2003) 3353.

[21] V.Q. Nguyen, M. Sadilek, J. Ferrier, A.J. Frank, F. Tureek, J. Phys. Chem. A 101 (1997) 3789.

[22] Because Ala is near the S–S bond at and near minimum-energy structures, it is thus likely to be able to effect TS electron transfer during the ca. $10-6$ s window of opportunity available to it.

[23] To test the degree of steric crowding, it would be useful to repeat the experiments carried out in the McLuckey lab using ECD rather than ETD. In ECD, the free electrons would not be as hindered in reaching the S–S bond site as is the azobenzene anion used in ETD.

[24] Geometrical considerations alone suggest these rates to vary with distance as R_{NS}^{-2}. It is on these geometrical considerations that we suggest these three rates will occur in the order $r_2 > r_1 > r_3$.

[25] If, in fact, initial electron transfer to the Ala (or TMAB-substituted Ala) suffers from steric hindrance, the yield of S–S cleavage in this species could be even further lowered.